



Published in final edited form as:

*Science*. 2013 March 22; 339(6126): 1445–1448. doi:10.1126/science.1231077.

## A Localized Wnt Signal Orients Asymmetric Stem Cell Division in Vitro

Shukry J. Habib<sup>1,2,\*</sup>, Bi-Chang Chen<sup>2</sup>, Feng-Chiao Tsai<sup>3</sup>, Konstantinos Anastassiadis<sup>4</sup>, Tobias Meyer<sup>3</sup>, Eric Betzig<sup>2</sup>, and Roel Nusse<sup>1,\*</sup>

<sup>1</sup>Department of Developmental Biology, Howard Hughes Medical Institute, Institute for Stem Cell Biology and Regenerative Medicine, Stanford University, 265 Campus Drive, Stanford, CA 94305, USA

<sup>2</sup>Janelia Farm Research Campus, 19700 Helix Drive, Ashburn, VA 20147, USA

<sup>3</sup>Department of Chemical and Systems Biology, Stanford University, Stanford, CA 94305, USA

<sup>4</sup>BIOTEC, Technische Universität Dresden Tatzberg 47-51, 01307 Dresden, Germany

### Abstract

Developmental signals such as Wnts are often presented to cells in an oriented manner. To examine the consequences of local Wnt signaling, we immobilized Wnt proteins on beads and introduced them to embryonic stem cells in culture. At the single-cell level, the Wnt-bead induced asymmetric distribution of Wnt- $\beta$ -catenin signaling components, oriented the plane of mitotic division, and directed asymmetric inheritance of centrosomes. Before cytokinesis was completed, the Wnt-proximal daughter cell expressed high levels of nuclear  $\beta$ -catenin and pluripotency genes, whereas the distal daughter cell acquired hallmarks of differentiation. We suggest that a spatially restricted Wnt signal induces an oriented cell division that generates distinct cell fates at predictable positions relative to the Wnt source.

---

Asymmetric cell division is a fundamental process involved in many aspects of stem cell biology and cancer (1), but insight into external cues that control asymmetric divisions is limited (2). Although much has been learned from examining asymmetric cell divisions in vivo (3–5), the complexity of tissues and the multiplicity of signals create challenges to understanding how localized growth factors affect cell behaviors at the single-cell level. Using in vitro studies, single cells and their divisions can be followed; however, growth factors that are added to the tissue medium present signals in a nonoriented way. To study how a given growth factor affects cell divisions or cell fates at the level of the individual cell, methods should be used to present purified signaling molecules in an oriented way.

Previously we found that Wnt3a protein maintains the self-renewal of several types of stem cells, including embryonic stem (ES) cells (6). Conversely, blocking endogenous Wnt signals made by ES cells leads to differentiation toward Epiblast stem cells (EpiSCs) (6). ES cells are grown in media supporting pluripotency that include conditions that globally activate Wnt signaling (called 2i) (7, 8) and induce ES cells to divide in mainly symmetrical

---

\*Corresponding author: rnusse@stanford.edu (R.N.); shabib@stanford.edu (S.J.H.).

Supplementary Materials

[www.sciencemag.org/cgi/content/full/339/6126/1445/DC1](http://www.sciencemag.org/cgi/content/full/339/6126/1445/DC1) Materials and Methods

Figs. S1 to S12

Movies S1 to S10

References (30–33)

patterns (9). Hence, ES cells could provide a useful experimental model for assessing how a local rather than a global Wnt signal might direct stem cell fate choices.

To examine the effect of a spatially localized Wnt signal on ES cells, we immobilized Wnt signals to beads and observed single cells with live imaging. Although Wnt3a maintains ES cell pluripotency (6), the Wnt5a protein, which commonly operates through a non- $\beta$ -catenin-dependent pathway (10), did not (figs. S1 and S8F), allowing us to use Wnt5a as a control. We chemically immobilized purified Wnt3a or Wnt5a proteins to beads (figs. S2A and S3A) and confirmed their biological activity (figs. S2, B to D, and S3, B and C). ES cells were plated at low density in the presence of leukemia inhibitory factor (LIF), and individual cells with a bead attached were followed by live cell microscopy as they divided. We examined the location of Wnt signaling components by antibody staining. In the presence of Wnt3a beads (Fig. 1A), but rarely with Wnt5a beads (fig. S4), the Wnt receptor LRP6 became asymmetrically localized to the side of the ES cell contacting the bead. Moreover, a Frizzled1-GFP (green fluorescent protein) fusion protein (fig. S5) and the adenomatous polyposis coli (APC) protein, a component of the  $\beta$ -catenin destruction complex, were detected in close proximity to the Wnt3a beads (Fig. 1A and fig. S6).

In ES cells contacting Wnt3a beads before division,  $\beta$ -catenin was distributed asymmetrically close to the bead, overlapping with the location of APC (Fig. 1A and fig. S6). During division,  $\beta$ -catenin was retained at high abundance in the prospective proximal daughter cell, both at the cell membrane and in the nucleus (Fig. 1B). The asymmetric distribution of these Wnt components was maintained after the cells divided: The daughter cell in proximity to the Wnt3a bead preserved high amounts of LRP6 and APC, in contrast to the lower amounts in the distal cell (Fig. 1C and fig. S6).

Wnt pathway components can interact with astral microtubules and other components of the mitotic spindle, including centrosomes (11, 12). We investigated the effect of Wnt beads on the asymmetric inheritance of the centrosomes by expressing tagged Centrin1 (a component of the centriole) and the appendage component Ninein (13, 14). Ninein marks the centrosome with the older centriole (13–15), whereas the other centrosome receives new centrioles that initially lack these structures. By the end of division, centrosomes in 78% of the cells ( $n = 18$ ) that were attached to Wnt3a beads had a high abundance of Ninein (Fig. 2, A and B), whereas the segregation of Ninein was almost random in the presence of the Wnt5a beads (54%;  $n = 15$ ). Thus, the association with Wnt3a beads correlates with the asymmetric inheritance of centrosomes.

Because centrosomes orient the mitotic spindle, we investigated whether Wnt beads direct the orientation of cell division and partitioning of chromosomes during mitosis (16). ES cells expressing a histone 2B–Venus chimeric protein to mark chromosomes (Fig. 2, C and D) were incubated with Wnt beads and monitored during mitosis by rapid three-dimensional imaging of living cells (17). In 75% of the dividing cells ( $n = 16$ ), the axis of mitotic division was oriented in line with the Wnt3a bead (Fig. 2C and movie S1), whereas only 12% of divisions were oriented toward Wnt5a control beads ( $n = 12$ ; Fig. 2D and movie S2).

We investigated the effect of localized Wnt signals on pluripotency gene expression, by using various ES reporter cells including cells expressing a Nanog–Venus fusion protein and GFP-based reporters for Rex1, Sox2, and Stella (18–21). Pluripotency proteins were also followed by antibody staining. The expression of Nanog, Rex1, and Stella has been shown to decline during ES cell differentiation (18–23). In dividing ES cells, we found that the transcriptional activities and protein abundance of the pluripotency markers were markedly higher in the Wnt3a-proximal daughter compared to the distal one (Fig. 3, A to C; fig. S7C; fig. S8, A to C; and fig. S9; and movies S3 to S6). Differences in gene expression levels were

detectable before cytokinesis was complete (Fig. 3B, at 140 min; fig. S9A(a), at 120 min; and fig. S9B(a), at 200 min). By contrast, in the presence of Wnt5a beads, the two daughters had similar levels of marker expression (Fig. 3C; fig. S7, A to C, fig. S8, D to F; and fig. S9; and movies S7 to S10). As might be expected, cells exposed to two Wnt3a beads at opposing ends divided symmetrically (fig. S10). As additional controls, we generated attenuated forms of Wnt3a, using Wnt3a beads that were treated after coupling with a range of concentrations of the reducing agent dithiothreitol, lowering the signaling activity of the beads in a dose-dependent manner (fig. S3, B and C). The potency of these beads in inducing asymmetric gene expression of the reporter Rex1-GFP was reduced commensurate with the remaining level of Wnt signaling (fig. S6). We also tested the activity of another signal implicated in the Wnt pathway; an active form of R-Spondin bound to beads (fig. S11A). There was no significant effect on asymmetric gene expression (Fig. 3C), possibly related to the behavior of R-Spondin *in vivo*, where it acts as a systemic rather than a local Wnt activator (24).

Under “standard” conditions, including feeder cells that can be source of Wnts or the 2i conditions, ES cells divide mainly symmetrically (6–9). We asked whether a global Wnt environment would be required for the symmetrical divisions that ES cells undergo. As a test, we perturbed Wnt signaling locally by applying the Wnt inhibitor Dickkopf (DKK) on beads (fig. S11B). Under these conditions, we found a significant number of divisions giving rise to asymmetric gene expression in the daughter cells, but in a manner opposite to that induced by the Wnt beads. With DKK-beads, the distal cell had higher expression of the pluripotency gene Rex1 than the proximal cell (Fig. 3C). We could rescue the effect of a local Wnt or Wnt inhibition by incubating the cells at the same time under the 2i conditions (7, 8), indicating that the asymmetry induced by Wnt3a or DKK beads was not a nonspecific perturbation of the cells (Fig. 3C). We argue, based on the asymmetric Wnt inhibition experiments, that uniform Wnt signaling is required for symmetric daughter cell fate.

The lower levels of pluripotency markers in the Wnt3a-distal daughter cell suggested that distal cells enter a differentiation program with hallmarks of EpiSCs (22). The pluripotency gene *Oct4* is expressed at similar levels in ES cells and EpiSCs (6, 25, 26). We observed symmetrical distribution of Oct4-Venus after cell division, either in the presence of Wnt3a or Wnt5a beads (Fig. 4, A and B). We assessed the expression of EpiSC markers, including Claudin6 (6, 25), which was higher in 60% of Wnt3a-distal cells (Fig. 4C) compared to Wnt5a distal cells (23% asymmetric expression; fig S12). H3K27me3 focal staining, a hallmark of an inactivated X chromosome in female ES cells (27), was detected in 57% of Wnt3a bead–distal ES cells after division (Fig. 4D). Thus, localized Wnt3a signal specifies that the Wnt3a-distal cell enters a differentiation program with hallmarks of EpiSC fate.

The findings reported here suggest a mechanism for external control of asymmetric stem cell division and differentiation. Specifically, a spatially localized Wnt signal orients the mitotic division plane of stem cells. Then, in the dividing cell, the Wnt signal produces an asymmetric distribution of Wnt signaling components, generating a “Wnt-on” proximal cell that maintains ES pluripotency and a “Wnt-off” distal cell that differentiates toward an EpiSC cell fate. Therefore, by orienting cell division, the Wnt signal positions the distal daughter cell out of its signaling range, leading to differentiation.

Although the protein distribution of Wnt signals in tissues is mostly unknown, a role for Wnts in setting up polarity is supported by findings made *in vivo*. Wnt signaling receptors in *Caenorhabditis elegans* and *Drosophila* distribute asymmetrically in cells that are exposed to local Wnt sources (28, 29). In *C. elegans*, the position of the P2 cell, which expresses Wnt, determines the polarity and divisional orientation of the neighboring EMS cell, leading to different fates of the EMS daughters (3–5). By growing single cells exposed to a

symmetry-breaking signal, we have developed a system that allows for precise real-time examination of processes involved in asymmetric cell divisions.

## Supplementary Material

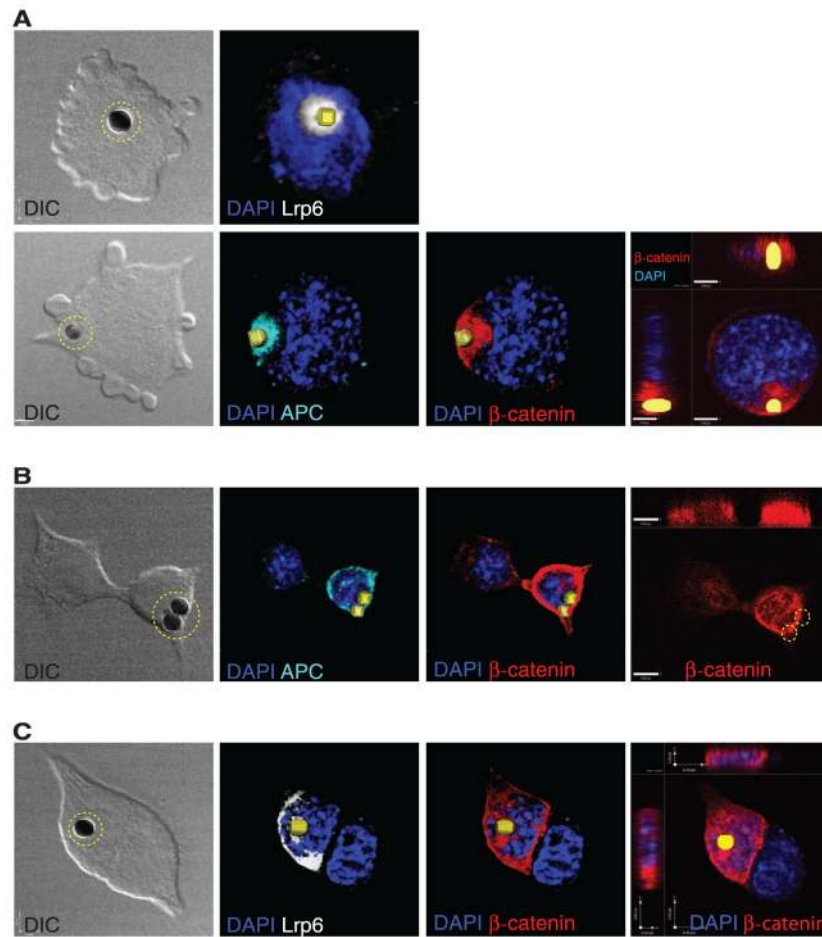
Refer to Web version on PubMed Central for supplementary material.

## Acknowledgments

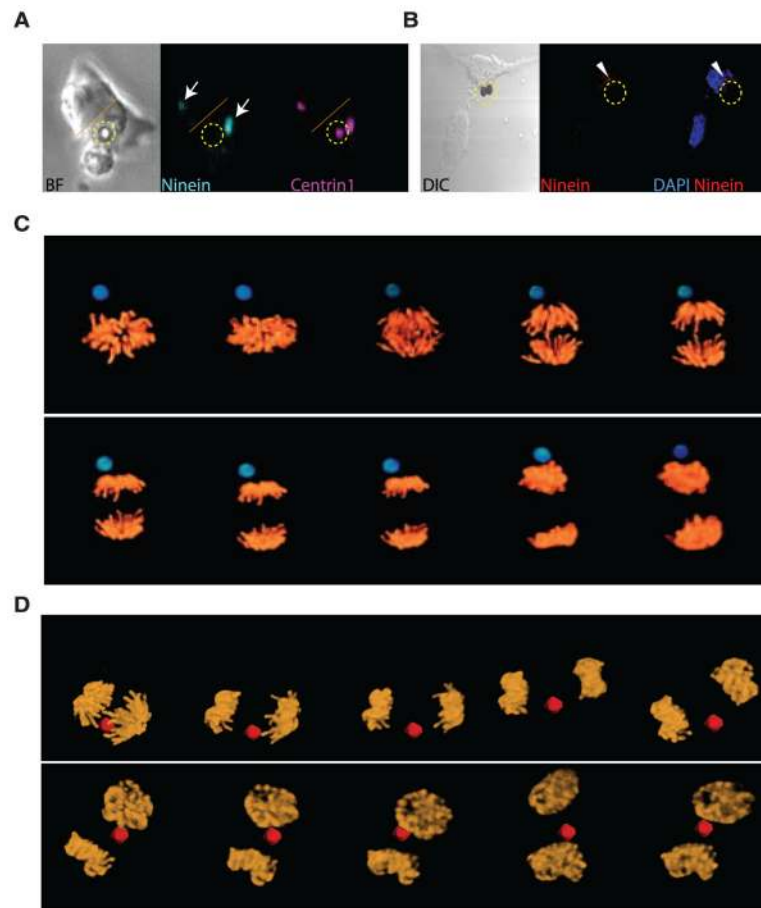
These studies were supported by the Howard Hughes Medical Institute and by grants RC1-00133-1, RB4-05825, and TR1-02149 from the California Institute for Regenerative Medicine to R.N.; by NIH grant GM063702 to T.M.; and by the Center for Regenerative Therapies Dresden and grant DFG-SPP1356 to K.A. We thank the Stanford Neuroscience Microscopy Service, supported by NIH NS069375. Patent applications are pending for the Bessel beam plane illumination microscopy (by E.B.) and for the Wnt, DKK, and R spondin1 immobilization technology and their applications (by S.J.H. and R.N.). We also thank M. Drukker, T. Schroeder, and T. Stearns for discussions. We appreciate discussions and comments on the manuscript by C. Logan and J. Nelson. S.J.H. was supported by a fellowship from the Deutsche Forschungsgemeinschaft (DFG) and a Siebel scholarship.

## References and Notes

1. Neumüller RA, Knoblich JA. *Genes Dev.* 2009; 23:2675. [PubMed: 19952104]
2. Werts AD, Goldstein B. *Semin Cell Dev Biol.* 2011; 22:842. [PubMed: 21807106]
3. Walston T, et al. *Dev Cell.* 2004; 7:831. [PubMed: 15572126]
4. Goldstein B, Takeshita H, Mizumoto K, Sawa H. *Dev Cell.* 2006; 10:391. [PubMed: 16516841]
5. Sugioka K, Mizumoto K, Sawa H. *Cell.* 2011; 146:942. [PubMed: 21925317]
6. ten Berge D, et al. *Nat Cell Biol.* 2011; 13:1070. [PubMed: 21841791]
7. Sato N, Meijer L, Skaltsounis L, Greengard P, Brivanlou AH. *Nat Med.* 2004; 10:55. [PubMed: 14702635]
8. Ying QL, et al. *Nature.* 2008; 453:519. [PubMed: 18497825]
9. Surani A, Tischler J. *Nature.* 2012; 487:43. [PubMed: 22763548]
10. Mikels AJ, Nusse R. *PLoS Biol.* 2006; 4:e115. [PubMed: 16602827]
11. Bahmanyar S, et al. *Genes Dev.* 2008; 22:91. [PubMed: 18086858]
12. Yamashita YM, Jones DL, Fuller MT. *Science.* 2003; 301:1547. [PubMed: 12970569]
13. Mogensen MM, Malik A, Piel M, Bouckson-Castaing V, Bornens M. *J Cell Sci.* 2000; 113:3013. [PubMed: 10934040]
14. Wang X, et al. *Nature.* 2009; 461:947. [PubMed: 19829375]
15. Bornens M. *Science.* 2012; 335:422. [PubMed: 22282802]
16. Yamashita YM, Fuller MT. *J Cell Biol.* 2008; 180:261. [PubMed: 18209101]
17. Planchon TA, et al. *Nat Methods.* 2011; 8:417. [PubMed: 21378978]
18. Payer B, et al. *Genesis.* 2006; 44:75. [PubMed: 16437550]
19. Toyooka Y, Shimamoto D, Murakami K, Takahashi K, Niwa H. *Development.* 2008; 135:909. [PubMed: 18263842]
20. Hayashi K, Lopes SM, Tang F, Surani MA. *Cell Stem Cell.* 2008; 3:391. [PubMed: 18940731]
21. Arnold K, et al. *Cell Stem Cell.* 2011; 9:317. [PubMed: 21982232]
22. Singh AM, Hamazaki T, Hankowski KE, Terada N. *Stem Cells.* 2007; 25:2534. [PubMed: 17615266]
23. Chambers I, et al. *Nature.* 2007; 450:1230. [PubMed: 18097409]
24. Kim KA, et al. *Science.* 2005; 309:1256. [PubMed: 16109882]
25. Tesar PJ, et al. *Nature.* 2007; 448:196. [PubMed: 17597760]
26. Guo G, et al. *Development.* 2009; 136:1063. [PubMed: 19224983]
27. Plath K, et al. *Science.* 2003; 300:131. [PubMed: 12649488]
28. Hilliard MA, Bargmann CI. *Dev Cell.* 2006; 10:379. [PubMed: 16516840]
29. Korkut C, et al. *Cell.* 2009; 139:393. [PubMed: 19837038]

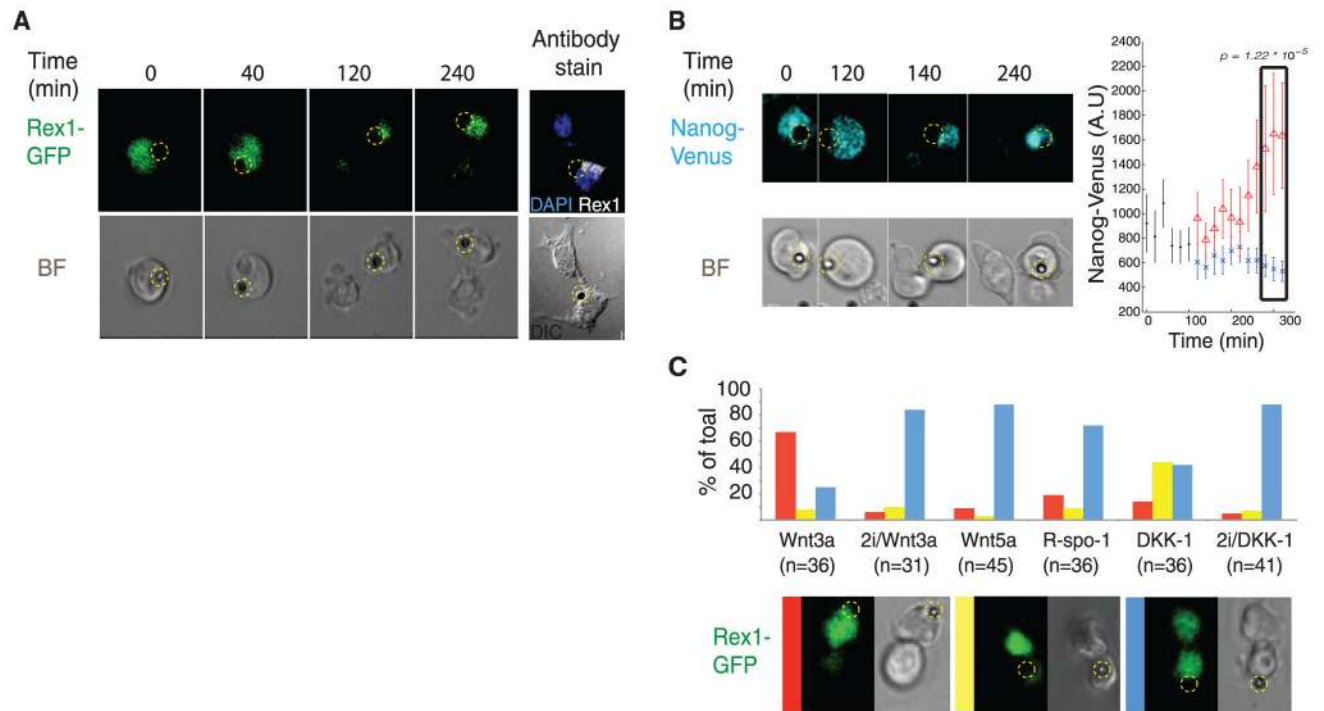


**Fig. 1.** Wnt3a beads induce asymmetric distribution of components of the Wnt/ $\beta$ -catenin pathway. Representative images of ES cells cocultured with Wnt3a beads (indicated by dashed yellow circle or reconstructed as a yellow square) and stained with antibodies to LRP6 (white), APC (cyan), and  $\beta$ -catenin (red). (A) Before division; (B) during division; (C) after division. The beads are 2.8  $\mu$ m. The far right panels show optical sections through the nucleus. DAPI, 4',6-diamidino-2-phenylindole; DIC, differential interference contrast.



**Fig. 2.** Asymmetric inheritance of centrosomes and the orientation of the plane of mitotic division. Time-lapse imaging of dividing single ES cells cocultured with Wnt3a beads (indicated by a dashed yellow circle) and (A) expressing enhanced green fluorescent protein (EGFP)–Ninein (cyan; arrows) and DsRedex–Centrin1 (magenta). Dotted orange line indicates the boundary between two cells. (B) Immunostaining for endogenous Ninein (arrowheads). BF: bright-field image. (C and D) Representative images from three-dimensional time-lapse microscopy of segregating chromosomes in ES cells expressing H2B–Venus that were cocultured with Wnt3a beads (blue) or Wnt5a beads (red).



**Fig. 3.**

Expression of the pluripotency genes Rex1 and Nanog during ES cell division. **(A)** Selected frames from time-lapse imaging of a dividing Rex-1 GFP reporter ES cell in the presence of a Wnt3a bead (indicated by a dashed yellow circle). The far right panel shows antibody staining for endogenous Rex-1 protein. **(B)** Selected frames from time-lapse imaging of a dividing Nanog-Venus reporter ES cell in the presence of a Wnt3a bead. Signal intensities of all frames were individually determined, and the mean  $\pm$  SD intensity values plotted. Red triangles represent signal intensities of the cell retaining contact with the bead after division. **(C)** Representative images of time-lapse microscopy of dividing Rex-1 GFP ES reporter cells cocultured in the presence of the indicated beads in 2i or 2i-free media. Cell divisions were classified based on the relative expression of GFP and plotted. Red bar: higher GFP amounts in the bead-proximal cell; yellow bar: higher amounts of GFP in the bead-distal cell; blue bar: similar amounts of GFP in either cell.

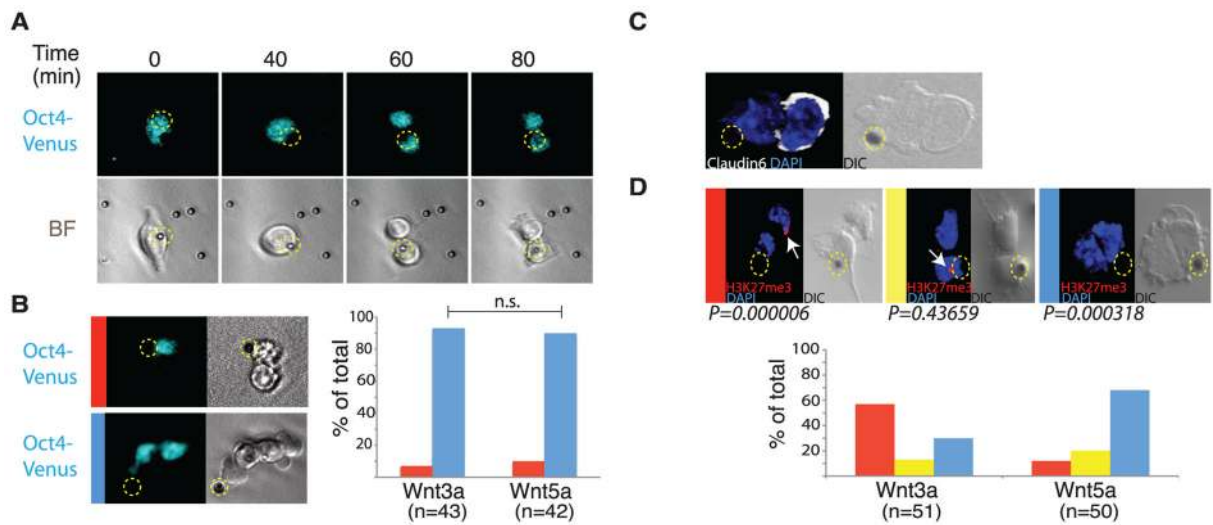


**Fig. 4.** Distal cells express markers of epiblast stem cell fate. **(A)** Selected frames from time-lapse imaging of a dividing Oct4-Venus reporter ES cell cocultured with a Wnt3a bead (indicated by a dashed yellow circle). **(B)** Divisions of Oct4-Venus ES cells cocultured with Wnt3a or Wnt5a beads were classified based on the relative expression of Venus, and plotted. Red bar: higher Venus abundance in the bead-proximal cell; blue bar: similar abundance of Venus in both cells. **(C)** Antibody staining for Claudin6 in an ES cell cocultured with a Wnt3a bead. **(D)** Representative images of antibody staining for H3K27me3 (arrows) in LF2 female ES cells cocultured with Wnt3a or Wnt5a beads. Dividing cells were classified based on location of the H3K27me3 stain, and plotted. Red bar: H3K27me3 stain in the bead-distal cell; yellow bar: H3K27me3 stain in the bead-proximal cell; blue bar: no H3K27me3 stain in any cell.